# Radiation signal accompanying the Schwinger effect

I. A. Aleksandrov [1,2] A. D. Panferov [3] and S. A. Smolyansky [3,4]

[1]*Department of Physics, Saint Petersburg State University, 199034 Saint Petersburg, Russia*
[2]*Ioffe Institute, 194021 Saint Petersburg, Russia*
[3]*Saratov State University, 410026 Saratov, Russia*
[4]*Tomsk State University, 634050 Tomsk, Russia*

The properties of the forced oscillations of virtual electron-positron plasma generated in vacuum under the action of a short laser pulse are considered. By calculating the density of the conduction and polarization currents within the quantum kinetic approach, we demonstrate the presence of plasma oscillations at the frequency of the external field and its odd harmonics. It is expected that radiation generated by these plasma oscillations can be observed outside the interaction region, for example, outside the focal spot of two counterpropagating laser beams, and can serve as an indicator of the Schwinger mechanism of electron-positron creation from vacuum.

## I. INTRODUCTION

Viewing vacuum not as a mere scene where material objects interact with each other was a necessary step towards a self-consistent quantum field theory. Nontrivial properties of the quantum vacuum manifest themselves, for instance, in the phenomenon of Schwinger pair production [1–3]. To observe this effect, one has to approach the regime of extremely large electric field strength $E_\mathrm{c} = m^2 c^3 / |e|\hbar \approx 1.3 \times 10^{16}$ V/cm ($m$ and $e < 0$ are the electron mass and charge, respectively). The possibility of reaching this value, albeit for a very short time, appears due to current developments of the technology for generating ultrahigh-power laser pulses. To achieve the critical value $E_\mathrm{c}$, it is necessary to ensure the energy flux density in the focal spot of the laser setup close to $2.3 \times 10^{29}$ W/cm$^2$. Presently, an intensity of about $10^{23}$ W/cm$^2$ ($E \approx 0.001E_\mathrm{c}$) is considered to be an attainable regime within a number of projects under construction and commissioned [4–8]. For the next-generation projects [9–13], the expected values of this parameter are in the range $10^{24}$–$10^{25}$ W/cm$^2$ ($E \approx 0.01E_\mathrm{c}$). Under these conditions, the question of setting up experiments takes on practical significance.

Usually, direct detection of positrons or detection of characteristic signatures of positron annihilation is considered as a way of observing the Schwinger effect. Now we possess detailed information on the dependence of the characteristics of primary pairs on the parameters of the active field. Basically, it can be argued that the possible directions of the emission of the primary particles and their energies can be predicted with high accuracy and resolution. This should prevent an unambiguous interpretation of the recorded events. However, there will also be a masking background arising due to cascade processes (see, e.g., Refs. [14–19]) involving primary particles themselves or inevitable impurities.

In this study, we use the quantum kinetic approach and show that the polarization of the vacuum state in the presence of a strong alternating electric field can manifest itself in the form of reemission of part of its energy both at its fundamental frequency and at its odd high-frequency harmonics. In particular, we will demonstrate that subcritical vacuum polarization results in the third harmonic in the radiation spectrum generated by virtual electrons and positrons.

This study complements recent investigations of the radiation process described by the tadpole QED diagram [20–25] (see also Refs. [26–28]). Our findings represent a next step towards understanding the polarization properties of quantum vacuum, which also give rise, for instance, to a remarkable phenomenon of vacuum birefringence (see, e.g., Refs. [29–31] and references therein). We underline that the process under consideration involves virtual particles excited by the external background and described in terms of macroscopic current densities.

The structure of this paper is the following. In Sec. II we briefly describe a theoretical framework based on the quantum kinetic equations. In Sec. III we discuss the temporal evolution of the conduction and polarization currents. Our main findings concerning quasiclassical radiation are presented in Sec. IV. In Sec. V we provide a summary and discuss conclusions. Throughout the text, we assume $c = \hbar = 1$.

## II. KINETIC EQUATION

For the description of the process of vacuum particle production at $t \to \infty$ and also of the intermediate quasiparticle excitations and polarization effects in a strong electric field, we will employ the kinetic equation (KE) for the case of a uniform linearly polarized electric field $E(t) = -\dot{A}(t)$ with a vector potential $A^\mu(t) = (0, 0, 0, A(t))$ [32–36] (for more details, see also Refs. [37,38]),

$$\dot{f}(\mathbf{p}, t) = \tfrac{1}{2}\lambda(\mathbf{p}, t) \int_{t_\mathrm{in}}^{t} dt' \lambda(\mathbf{p}, t')[1 - 2f(\mathbf{p}, t')] \cos\theta(t, t'),$$

$$(1)$$

where $f(\mathbf{p}, t)$ is the quasiparticle distribution function,

$$\lambda(\mathbf{p}, t) = \frac{eE(t)\varepsilon_\perp}{\varepsilon^2(\mathbf{p}, t)}, \qquad (2)$$

$$\theta(t, t') = 2 \int_{t'}^{t} d\tau\, \varepsilon(\mathbf{p}, \tau). \qquad (3)$$

Here $\lambda$ is the amplitude of the vacuum transitions and $\theta$ is a high-frequency phase describing the vacuum oscillations which are modulated by the external field. The quasienergy $\varepsilon(\mathbf{p}, t) = \sqrt{\varepsilon_\perp^2 + P^2}$ is defined by means of transverse energy $\varepsilon_\perp = \sqrt{m^2 + p_\perp^2}$ and longitudinal kinetic quasimomentum $P = p_\parallel - eA(t)$. Here $p_\perp = |\mathbf{p}_\perp|$ is the magnitude of the vector $\mathbf{p}_\perp$ perpendicular to the field direction and $p_\parallel = p_3$ is the momentum component parallel to the external field.

We consider Eq. (1) with zero initial conditions, i.e., $f(\mathbf{p}, t_{\mathrm{in}}) = 0$, and set $E(t_{\mathrm{in}}) = 0$ and $A(t_{\mathrm{in}}) = A_{\mathrm{in}}$. It is also assumed that the electric field is switched off in the *out* state $[E(t \to \infty) = 0$ and $A(t \to \infty) = A_{\mathrm{out}}$ can differ from $A_{\mathrm{in}}]$.

The non-Markovian integro-differential equation (1) is equivalent to a system of three ordinary differential equations

$$\dot{f} = \tfrac{1}{2}\lambda u, \quad \dot{u} = \lambda(1 - 2f) - 2\varepsilon v, \quad \dot{v} = 2\varepsilon u, \qquad (4)$$

where $u(\mathbf{p}, t)$ and $v(\mathbf{p}, t)$ are auxiliary functions describing vacuum polarization effects. Equations (4) are to be considered with the initial conditions $f(\mathbf{p}, t_{\mathrm{in}}) = u(\mathbf{p}, t_{\mathrm{in}}) = v(\mathbf{p}, t_{\mathrm{in}}) = 0$. This system is convenient for a numerical investigation of the problem.

The kinetic equation (1) and the equivalent system (4) are exact within the tree level of QED, i.e., when one neglects the interaction with a quantized part of the electromagnetic field. They were obtained within several nonperturbative approaches: Bogoliubov transformation [33–35,37], QED equations in the Wigner representation [32,39], the Foldy-Wouthuysen method [36,40], and a general KE system describing pair production in a classical background field [38].

The density of the quasiparticles, i.e., the number of quasiparticles per unit volume, reads

$$n(t) = 2 \int [dp] f(\mathbf{p}, t), \qquad (5)$$

where the factor 2 corresponds to spin degeneracy and $[dp] \equiv d^3 p/(2\pi)^3$. The total current density can be decomposed into the sum of the conduction and polarization components [41],

$$j(t) = j^{\mathrm{cond}}(t) + j^{\mathrm{pol}}(t), \qquad (6)$$

where

$$j^{\mathrm{cond}}(t) = 2e \int [dp] \frac{P}{\varepsilon(\mathbf{p}, t)} f(\mathbf{p}, t), \qquad (7)$$

$$j^{\mathrm{pol}}(t) = -e \int [dp] \frac{\varepsilon_\perp}{\varepsilon(\mathbf{p}, t)} u(\mathbf{p}, t). \qquad (8)$$

According to Eq. (8), the function $u(\mathbf{p}, t)$ can be interpreted as a current polarization function. The function $v(\mathbf{p}, t)$ determines the energy density of the vacuum polarization [37,38]. Both of these components originate from single-particle anomalous correlation functions.

Let us discuss the convergence of the integrals in Eqs. (7) and (8). Assuming that $p \gg m$, i.e., $\varepsilon \gg m$, one can demon-

strate that the asymptotic behaviors of the functions $f(\mathbf{p}, t)$ and $u(\mathbf{p}, t)$ read [42]

$$f \simeq f_4 = \frac{1}{16} \left( \frac{\lambda}{\varepsilon} \right)^2, \qquad (9)$$

$$u \simeq u_3 = \frac{1}{4\varepsilon} \frac{d}{dt} \left( \frac{\lambda}{\varepsilon} \right), \qquad (10)$$

where the subscripts indicate the order of the corresponding terms within the power expansion with respect to $m/\varepsilon \ll 1$. From this it follows that the conduction current (7) is already well defined, whereas the integral in Eq. (8) possesses a logarithmic divergence in the ultraviolet domain and should be regularized according to the subtraction procedure $u(t) \to u(t) - u_3(t)$ [42]. In what follows, we will always take into account this counterterm providing finite values of the polarization current, which will be denoted by $j_R^{\mathrm{pol}}(t)$.

According to the KEs (1) and (4), the distribution function $f(\mathbf{p}, t)$ and the vacuum polarization functions $u(\mathbf{p}, t)$ and $v(\mathbf{p}, t)$ incorporate temporal oscillations with the characteristic frequency of the external field (low frequency) and with the doubled frequency of the vacuum oscillations $2\sqrt{m^2 + \mathbf{p}^2}$ (high frequency) depending on the momentum $\mathbf{p}$. Integrating the macroscopic densities (5), (7), and (8) over momentum space flattens the high-frequency oscillations, making the results slowly varying with $t$ and more representative.

Finally, we note that within a period of the external field action, one can represent the total current (6) as a sum of the conduction and polarization components only formally as these cannot be distinguished experimentally. Basically, the vacuum polarization effects dominate in the densities mentioned above. In what follows, we will examine these effects by analyzing the currents (7) and (8).

### III. PARTICLE DENSITY AND CURRENTS

We consider the external electric background in the following form:

$$E(t) = E_0 \cos \Omega t\, e^{-t^2/2\tau^2}. \qquad (11)$$

Below we will also use the parameter $\sigma = \Omega\tau$, which is a dimensionless measure of the characteristic duration $\tau$ of the pulse governing the number of carrier cycles. In this case, the initial time instant tends to minus infinity, $t_{\mathrm{in}} \to -\infty$.

The expression (11) mimics the focal spot of two counter-propagating high-intensity laser pulses. We treat the external field as locally uniform in space since the qualitative character of our results does not change if the spatial inhomogeneities are taken into account (in Ref. [25] it was demonstrated that the field can be considered locally constant up to the frequency $\omega \gtrsim 0.5\, m$, which is satisfied in our investigation).

Our goal is to investigate the temporal behavior of the number density of quasiparticles (5) and current densities (7) and (8) during the action of the external electric pulse (11). Unfortunately, for optical and near-infrared frequencies this task is beyond the present computational capabilities, so we will work within the hard-x-ray domain. We expect that the main findings of this study will also provide correct qualitative predictions in the region of lower frequencies. In our
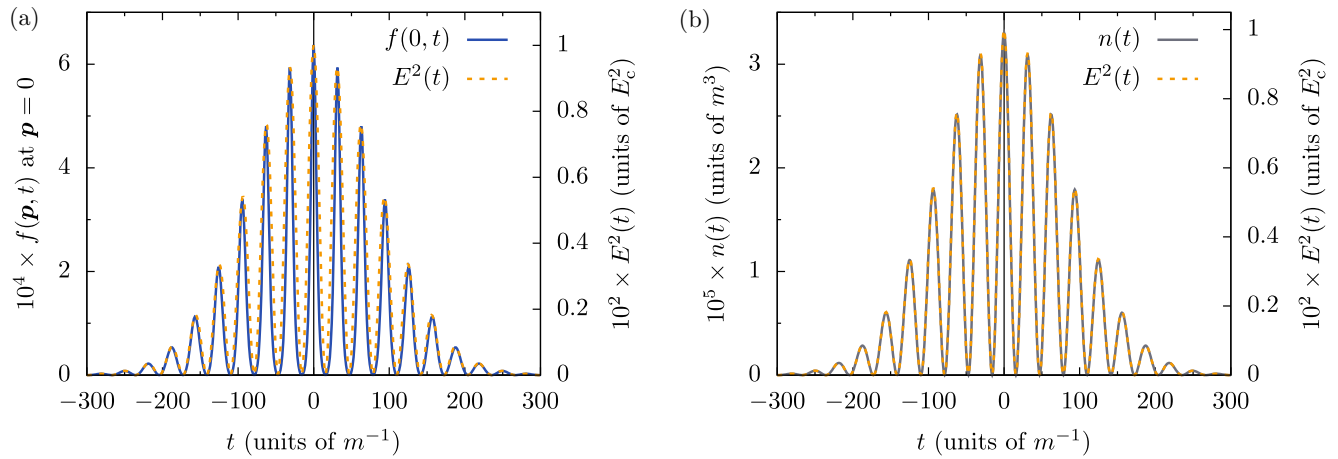
FIG. 1. (a) Distribution function $f(\mathbf{p}, t)$ at $\mathbf{p} = 0$ and (b) pair density (5) as functions of time together with the square of the external field strength $E(t)$. The field parameters are $E_0 = 0.1E_c$, $\Omega = 0.1\,m$, and $\sigma = 12$. The curve $E^2(t)$ almost exactly reproduces the other two curves.

simulations, the external field frequency corresponds to the photon energy of 51 keV ($\Omega = 0.1\,m$).

The problem is solved in two stages. In the first stage, we calculate the distribution $f(\mathbf{p}, t)$ according to the KE (1) and then, in the second stage, we evaluate the integrals (5), (7), and (8). The first stage is the most laborious since the function $f(\mathbf{p}, t)$ is defined in four-dimensional space. By solving the system of equations (4), one can obtain its temporal dependence only for a given set of parameters $\{p_1, p_2, p_3\}$. However, the axial symmetry reduces the dimension of the problem, so we assume $p_2 = 0$, leaving $p_1$ and $p_3$ as the transverse and longitudinal projections of the particle momentum, respectively ($p_1 = p_\perp$ and $p_3 = p_\parallel$).

Our calculations were carried out for $E_0 = 0.1E_c$. Although the energy of the external-field quanta amounts only to 51 keV, with such a high intensity, it turns out that the virtual electrons or positrons can gain about ten times more energy. Accordingly, the functions $f(\mathbf{p}, t)$, $u(\mathbf{p}, t)$, and $v(\mathbf{p}, t)$ were computed within the domain $0 \leqslant p_1 \leqslant p_{\text{cut}}$ and $-p_{\text{cut}} \leqslant p_3 \leqslant p_{\text{cut}}$, where $p_{\text{cut}} = 10.0\,m$. In the second stage, the integral characteristics, i.e., the number density (5) and currents (7) and (8), were calculated at each step of the temporal grid

containing 1000 points within the laser pulse support, which provided a high temporal resolution.

Figure 1 allows one to compare the temporal evolution of the distribution function at $\mathbf{p} = 0$ with the behavior of the pair number density (5). In these graphs we also depict the temporal dependence of the square of the field strength (11) in order to demonstrate that the particle density evolution is qualitatively similar to $E^2(t)$ [43]. The high-frequency oscillations become visible when one employs a logarithmic scale.

The temporal dependence of the conduction and polarization currents is displayed in Fig. 2. The results for the conduction current were obtained using the definition (7). The polarization current was calculated in accordance with Eq. (8), taking into account the counterterm (10) for regularization. First, one observes that the polarization current is about two orders of magnitude larger than the conduction one. Second, the conduction current exhibits a much more complicated temporal behavior containing double spikes of alternating direction [Fig. 2(a)]. The evolution of the polarization current is simpler [see Fig. 2(b)]: Its temporal dependence $j_R^{\text{pol}}(t)$ approximately reproduces a rescaled plot of $E(t)$ [Eq. (11)] shifted by $\Delta t = \pi/2\Omega$.
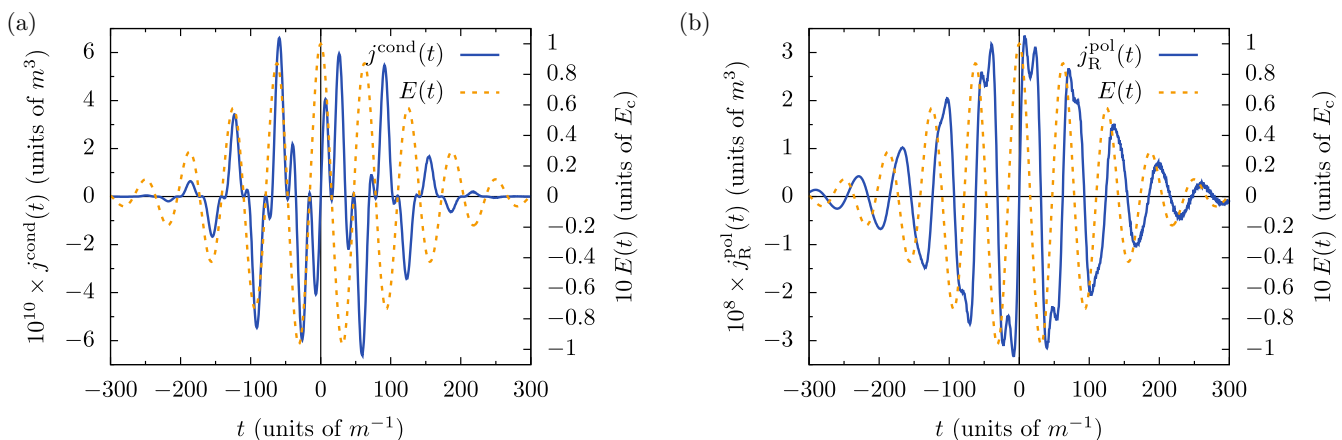


FIG. 2. Temporal dependence of (a) the conduction current and (b) the polarization current together with the external field strength $E(t)$. The field parameters are $E_0 = 0.1E_c$, $\Omega = 0.1\,m$, and $\sigma = 12$.
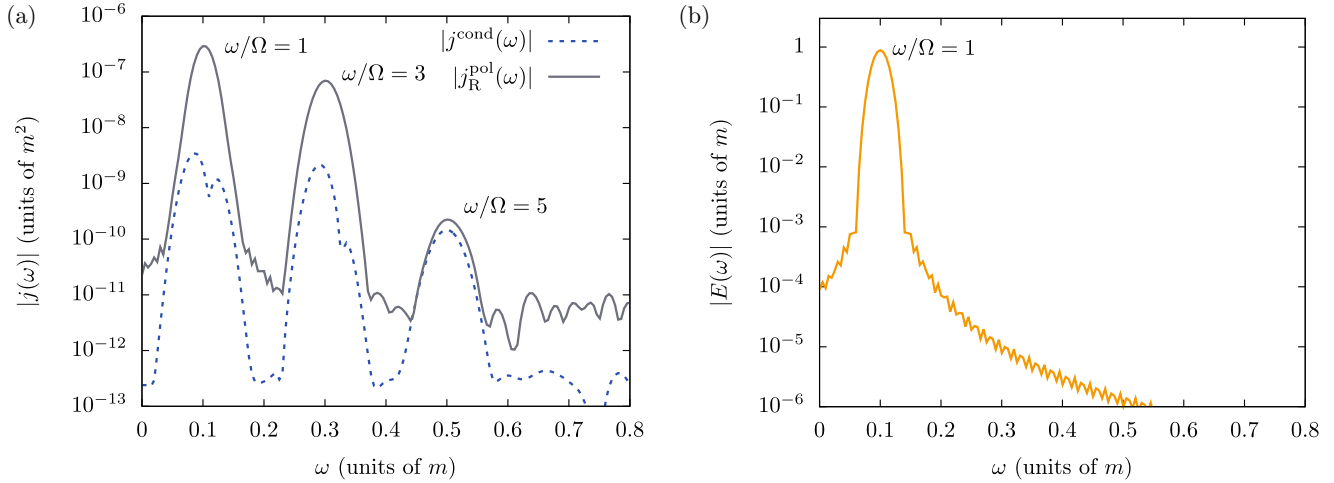
FIG. 3. Spectrum of (a) the conduction and polarization currents and (b) the external field $E(t)$. The field parameters are $E_0 = 0.1 E_c$, $\Omega = 0.1\,m$, and $\sigma = 12$.

The main part of the present study is devoted to the analysis of the spectral content of the calculated currents. In order to investigate this issue and perform the corresponding calculations, we utilized the `Periodogram` standard routines of *Mathematica* [44]. For better visibility of the results, we averaged the data from the partitions of the original list and smoothed the values with a window function of the Hann type. The resulting absolute values are presented in Fig. 3(a). Both curves clearly demonstrate the presence of higher odd harmonics ($\omega/\Omega = 1, 3, 5, \dots$). The third harmonic of the polarization current is well pronounced and is about two orders of magnitude larger than that of the conduction current. For the fifth harmonic, the amplitudes of the currents turn out to be very close in magnitude. For comparison, in Fig. 3(b) we depict an analogous Fourier transform of the external field (11) in which there are obviously no additional harmonics. This emphasizes that the appearance of high-frequency harmonics in the generated currents is a result of a complex nonlinear response of the physical vacuum. Our results qualitatively coincide with the findings presented in Refs. [25–28] and obtained by means of different techniques.

## IV. BACKREACTION PROBLEM AND RADIATION

The virtual electron-positron plasma (VEPP) currents generate the internal electric field $E_{\text{int}}(t)$, which obeys Maxwell's equation

$$\dot{E}_{\text{int}}(t) = -j(t) = -j^{\text{cond}}(t) - j_R^{\text{pol}}(t). \qquad (12)$$

The currents $j^{\text{cond}}(t)$ and $j_R^{\text{pol}}(t)$ should now be governed by a combined action of the external and internal fields, i.e., by the effective field $E_{\text{eff}}(t) = E(t) + E_{\text{int}}(t)$. The backreaction problem requires a self-consistent description of the KE (1) [or the KE system (4)] and Eq. (12) (see Refs. [35,41] and references therein).

Here we are interested in the spectral energy density of the plasma oscillations

$$w(\omega) = \frac{1}{8\pi}|E_{\text{int}}(\omega)|^2 = \frac{1}{8\pi\omega^2}|j(\omega)|^2 \qquad (13)$$

that follows from Eq. (12). The behavior of this function is shown in Fig. 4(a) for four different values of the field amplitude $E_0$ ($\Omega = 0.1\,m$ and $\sigma = 12$). The peak at the fundamental frequency of the external field and the third harmonic are well observed. There are signs of odd harmonics of higher orders, but for quantitative estimates of their characteristics, the data available at our disposal are not sufficiently accurate.

To assess the response of the physical vacuum to the action of the external field, let us consider the ratio of the spectral energy density of the plasma field (13) for the fundamental and third harmonics to the spectral energy density of the external field. Namely, we will explore here the relative brightness of the harmonics,

$$B_1(E_0) = \frac{|E_{\text{int}}(\Omega)|^2}{|E(\Omega)|^2}, \quad B_3(E_0) = \frac{|E_{\text{int}}(3\Omega)|^2}{|E(\Omega)|^2}, \qquad (14)$$

depending on the external field amplitude.

The results for the range $0.05 \leqslant E_0/E_c \leqslant 0.3$ are shown in Fig. 4(b). If the external field is present within a finite spatial region, the inner plasma field can escape from this domain, so one is able to detect the corresponding radiation far from the active area. Of course, at the fundamental frequency of the external field, its energy absolutely dominates $|E_{\text{int}}(\Omega)|^2 \ll |E(\Omega)|^2$. However, the direction of propagation of the rays that form this field is strictly determined. Within the KE formalism, the problem of extracting the angular distribution of the radiation flux generated by the plasma field is very difficult and beyond the scope of this study. It can only be noted that this radiation will be concentrated in a plane perpendicular to the plane of the polarization of the primary rays since the external and internal electric fields are collinear. However, there is no clear reason to believe that this secondary radiation will go strictly along the propagation line of the beams forming the focal spot (cf. Ref. [21]). Therefore, the results presented indicate that approaching the critical field strength in the focal spot should lead to the scattering of a (very small) part $B_1$ of the energy of the primary beams at sufficiently large angles. It can be noted that such scattering can be regarded as an analog of Thompson scattering of photons by free charges. However, in this case, the charge carriers are
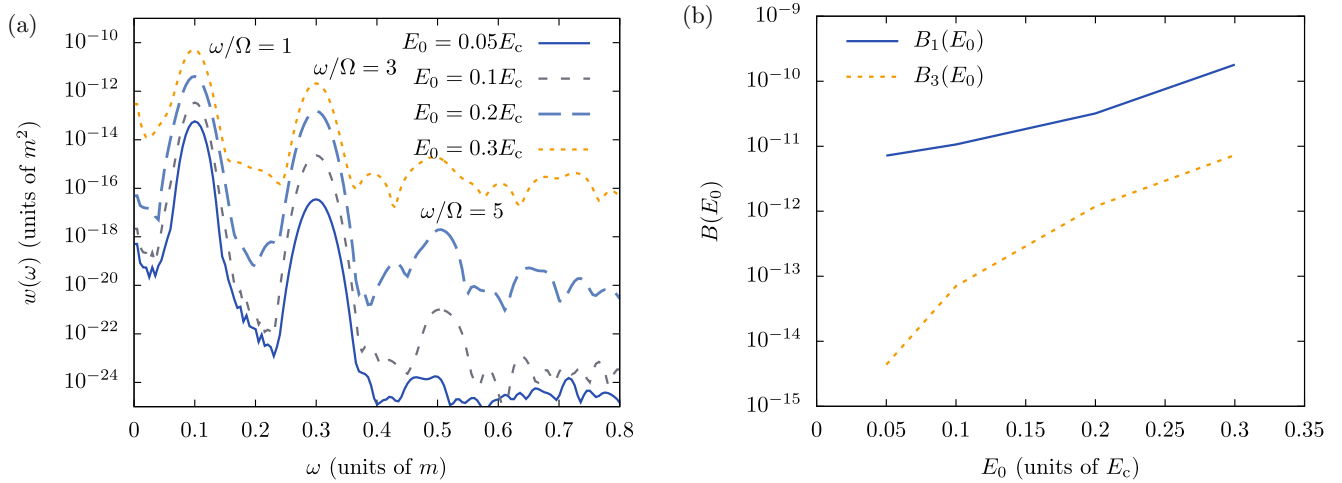
FIG. 4. (a) Spectral energy density (13) of the VEPP oscillations for $E_0 = 0.05E_c$, $0.1E_c$, $0.2E_c$, and $0.3E_c$ and (b) the relative brightness $B_1$ and $B_3$ defined in Eq. (14) as a function of $E_0$ according to the data. The other field parameters are $\Omega = 0.1\,m$ and $\sigma = 12$.

virtual electrons and positrons, the role of which becomes noticeable in near-critical fields. The presence of high-frequency harmonics in plasma radiation can be considered as one more firm indication of the nonlinear vacuum polarization effects in a strong field preceding plasma creation.

The absence of even harmonics in the spectra of the currents is a consequence of the maximal space-time symmetry of the physical vacuum as an active medium and is in accordance with the general theory of the response of nonlinear systems to external perturbations [45]. We also point out that quantum photon emission due to absorption of an even number of external-field quanta is also prohibited according to Furry's theorem [46]. Nevertheless, this process becomes possible if there are two outgoing photons instead of one. Then after the absorption of $2n$ external-field quanta with the frequency $\Omega$, the two photons can have the frequency $n\Omega$ each and $n$ can be odd [26]. However, this process will be suppressed by the additional factor $\alpha \approx 1/137$ and powers of $E_0/E_c$.

## V. CONCLUSION

A characteristic feature of nonequilibrium VEPP generated from vacuum under the action of intense external fields is the appearance of strong electric currents and the corresponding inner-plasma electromagnetic fields (the backreaction effect [35,41]). Such phenomena can be described either in terms of the tadpole QED diagram [20–28] or in the framework of a specific kinetic theory, as in the present study, predicting quasiclassical radiation. These two approaches are closely related: In the QED tadpole diagram the wave function of the outgoing photon is contracted with a loop which corresponds to the mean value of the current operator. Therefore, the spectral analysis of the current allows one to describe the process of photon emission. On the other hand, evaluating the mean value of the current operator in terms of the functions involved in the KEs (1) and (4), one exactly obtains the expressions (7) and (8). This fact represents a justification for our approach using the quasiparticle densities at the intermediate time interval, where the interpretation of the kinetic functions may be uncertain. We also point out that this formalism does not

incorporate quantum radiation due to annihilation of the $e^+e^-$ pairs in plasma (see Ref. [47]). Another source of radiation is the process of photon emission accompanying production of $e^+e^-$ pairs (see, e.g., Fig. 1 in Ref. [25]). The first steps in studying this mechanism were taken in Refs. [25,26,48,49]. However, this radiation channel corresponds to the emission of *soft* photons, i.e., it is responsible for a different part of the spectrum and thus does not alter the findings discussed in the present paper. Note also that real electrons and positrons can also emit photons via Thomson or Compton scattering (see, e.g., Ref. [50]). As we assume that the initial state does not contain any real particles, this radiation can only occur after the external field produces and accelerates pairs. Accordingly, in the (near) subcritical regime, this emission channel will not obscure the presence of odd harmonics in the radiation spectrum.

We also point out that vacuum harmonic generation or frequency mixing can occur in a background magnetic field [51] (see also Refs. [52,53] and references therein) and due to the four-wave interaction or similar processes (see, e.g., Refs. [53–60]).

The present investigation was motivated, on the one hand, by the previous work of Smolyansky *et al.* [61] on the nonperturbative kinetic description of excitations in graphene under the action of an external time-dependent electric field and, on the other hand, by studies [62–64] where both theoretical and experimental investigations of the radiation processes in graphene in optical and infrared domains were carried out.

In this study, it was shown that under the action of a short linearly polarized laser pulse with a high energy density, plasma oscillations are excited in the physical vacuum. Their spectrum contains the fundamental frequency of the external field and its high-frequency harmonics. It is expected that these vibrations cause additional radiation that escapes from the spatial region where the external laser fields are localized. The detection of this radiation and the observation of the third harmonic will convincingly indicate that the effects of vacuum polarization within strong-field QED take place in such a process, that is, it approaches the critical regime where the

production of electron-positron pairs should become possible. Let us underline the fact that the results obtained are of a rather general and stable character with respect to the specific choice of the external-field setting. For example, the same conclusion can be drawn in the case of a circularly polarized field as the physical vacuum can be regarded as a homogeneous isotropic active medium with a nonlinear response. Moreover, according to our data, the properties of the additional radiation are qualitatively independent of the Keldysh parameter $\gamma = m\Omega/|eE_0|$, which obeys $\gamma \ll 1$ in the tunneling (Schwinger) regime and $\gamma \gg 1$ in the perturbative (multi-

photon) regime, provided the external-field frequency $\Omega$ is well defined (in this paper, we presented the results for $\gamma = 0.3$–$2.0$).

[1] F. Sauter, Z. Phys. **69**, 742 (1931).

[2] W. Heisenberg and H. Euler, Z. Phys. **98**, 714 (1936).

[3] J. Schwinger, Phys. Rev. **82**, 664 (1951).

[4] J. P. Zou, C. Le Blanc, D. N. Papadopoulos, G. Chériaux, P. Georges, G. Mennerat, F. Druon, L. Lecherbourg, A. Pellegrina, P. Ramirez *et al.*, High Power Laser Sci. Eng. **3**, e2 (2015).

[5] S. Weber, S. Bechet, S. Borneis, L. Brabec, M. Bučka, E. Chacon-Golcher, M. Ciappina, M. DeMarco, A. Fajstavr, K. Falk *et al.*, Matter Rad. Extremes **2**, 149 (2017).

[6] N. V. Zamfir, Eur. Phys. J. Spec. Top. **223**, 1221 (2014).

[7] X. Zeng, K. Zhou, Y. Zuo, Q. Zhu, J. Su, X. Wang, X. Wang, X. Huang, X. Jiang, D. Jiang, Y. Guo, N. Xie, S. Zhou, Z. Wu, J. Mu, H. Peng, and F. Jing, Opt. Lett. **42**, 2014 (2017).

[8] J. H. Sung, H. W. Lee, J. Y. Yoo, J. W. Yoon, C. W. Lee, J. M. Yang, Y. J. Son, Y. H. Jang, S. K. Lee, and C. H. Nam, Opt. Lett. **42**, 2058 (2017).

[9] D. D. Meyerhofer, S. W. Bahk, J. Bromage, D. H. Froula, D. Haberberger, S. X. Hu, B. E. Kruschwitz, R. L. McCrory, J. F. Myatt, P. M. Nilson, J. B. Oliver, C. Stoeckl, W. Theobald, L. J. Waxer, and J. D. Zuegel, Bull. Am. Phys. Soc. **59**, UO5.006 (2014).

[10] B. Shen, Z. Bu, J. Xu, T. Xu, L. Ji, R. Li, and Z. Xu, Plasma Phys. Contr. Fusion **60**, 044002 (2018).

[11] J. Kawanaka, K. Tsubakimoto, H. Yoshida, K. Fujioka, Y. Fujimoto, S. Tokita, T. Jitsuno, N. Miyanaga, and Gekko-EXA Design Team, J. Phys.: Conf. Ser. **688**, 012044 (2016).

[12] G. A. Mourou, G. Korn, W. Sandner, and J. L. Collier, *Extreme Light Infrastructure: Science and Technology with Ultra-Intense Lasers* (THOSS Media GmbH, Berlin, 2011).

[13] A. V. Bashinov, A. A. Gonoskov, A. V. Kim, G. Mourou, and A. M. Sergeev, Eur. Phys. J. Spec. Top. **223**, 1105 (2014).

[14] A. R. Bell and J. G. Kirk, Phys. Rev. Lett. **101**, 200403 (2008).

[15] A. M. Fedotov, N. B. Narozhny, G. Mourou, and G. Korn, Phys. Rev. Lett. **105**, 080402 (2010).

[16] E. N. Nerush, I. Y. Kostyukov, A. M. Fedotov, N. B. Narozhny, N. V. Elkina, and H. Ruhl, Phys. Rev. Lett. **106**, 035001 (2011).

[17] N. V. Elkina, A. M. Fedotov, I. Y. Kostyukov, M. V. Legkov, N. B. Narozhny, E. N. Nerush, and H. Ruhl, Phys. Rev. ST Accel. Beams **14**, 054401 (2011).

[18] N. B. Narozhny and A. M. Fedotov, Phys. Usp. **58**, 95 (2015).

[19] T. Grismayer, M. Vranic, J. L. Martins, R. A. Fonseca, and L. O. Silva, Phys. Rev. E **95**, 023210 (2017).

[20] F. Karbstein and R. Shaisultanov, Phys. Rev. D **91**, 113002 (2015).

[21] H. Gies, F. Karbstein, and C. Kohlfürst, Phys. Rev. D **97**, 036022 (2018).

[22] B. King, H. Hu, and B. Shen, Phys. Rev. A **98**, 023817 (2018).

[23] A. Blinne, H. Gies, F. Karbstein, C. Kohlfürst, and M. Zepf, Phys. Rev. D **99**, 016006 (2019).

[24] F. Karbstein, A. Blinne, H. Gies, and M. Zepf, Phys. Rev. Lett. **123**, 091802 (2019).

[25] I. A. Aleksandrov, G. Plunien, and V. M. Shabaev, Phys. Rev. D **100**, 116003 (2019).

[26] A. Di Piazza, K. Z. Hatsagortsyan, and C. H. Keitel, Phys. Rev. D **72**, 085005 (2005).

[27] A. M. Fedotov and N. B. Narozhny, Phys. Lett. A **362**, 1 (2007).

[28] N. B. Narozhny and A. M. Fedotov, Laser. Phys. **17**, 350 (2007).

[29] F. Karbstein, H. Gies, M. Reuter, and M. Zepf, Phys. Rev. D **92**, 071301(R) (2015).

[30] F. Karbstein and C. Sundqvist, Phys. Rev. D **94**, 013004 (2016).

[31] F. Karbstein, Phys. Rev. D **98**, 056010 (2018).

[32] I. Bialynicki-Birula, P. Górnicki, and J. Rafelski, Phys. Rev. D **44**, 1825 (1991).

[33] A. A. Grib, S. G. Mamaev, and V. M. Mostepanenko, *Quantum Vacuum Effects in Strong Fields* (Friedmann Laboratoty, St. Petersburg, 1994).

[34] S. M. Schmidt, D. Blaschke, G. Röpke, S. A. Smolyansky, A. V. Prozorkevich, and V. D. Toneev, Int. J. Mod. Phys. E **7**, 709 (1998).

[35] Y. Kluger, E. Mottola, and J. M. Eisenberg, Phys. Rev. D **58**, 125015 (1998).

[36] V. N. Pervushin and V. V. Skokov, Acta Phys. Polon. B **37**, 2587 (2006).

[37] D. B. Blaschke, S. A. Smolyansky, A. D. Panferov, and L. Juchnowski, in *Proceedings of the Helmholtz International Summer School 2016 (HQ 2016): Quantum Field Theory at the Limits: From Strong Fields to Heavy Quarks, Dubna, Russia*, edited by A. Ali, D. Blaschke, A. Issadykov, and M. Ivanov (Verlag Deutsches Elektronen-Synchrotron, Hamburg, 2017).

[38] I. A. Aleksandrov, V. V. Dmitriev, D. G. Sevostyanov, and S. A. Smolyansky, Eur. Phys. J. Spec. Top. **229**, 3469 (2020).

[39] F. Hebenstreit, R. Alkofer, and H. Gies, Phys. Rev. D **82**, 105026 (2010).

[40] A. M. Fedotov, E. G. Gelfer, K. Y. Korolev, and S. A. Smolyansky, Phys. Rev. D **83**, 025011 (2011).

[41] J. C. R. Bloch, V. A. Mizerny, A. V. Prozorkevich, C. D. Roberts, S. M. Schmidt, S. A. Smolyansky, and D. V. Vinnik, Phys. Rev. D **60**, 116011 (1999).

[42] S. G. Mamaev and N. N. Trunov, Yad. Fiz. **30**, 1301 (1979) [Sov. J. Nucl. Phys. **30**, 677 (1979)].

[43] K. Y. Kravtcov, V. V. Dmitriev, S. A. Levenets, A. D. Panfyorov, S. A. Smolyansky, L. Yukhnovsky, and D. B. Blaschke, in *Proceedings of the Saratov Fall Meeting 2017: Laser Physics and Photonics XVIII and Computational Biophysics and Analysis of Biomedical Data IV, Saratov, Russian Federation*, edited by V. L. Derbov and D. E. Postnov (SPIE, Bellingham, 2018), Vol. 10717.

[44] Mathematica (Wolfram Research, Inc., Champaign, 2016), Version 11.0.

[45] Y. R. Shen, *The Principles of Nonlinear Optics* (Wiley, New York, 2002).

[46] W. H. Furry, Phys. Rev. **51**, 125 (1937).

[47] D. B. Blaschke, V. V. Dmitriev, G. Röpke, and S. A. Smolyansky, Phys. Rev. D **84**, 085028 (2011).

[48] A. Otto and B. Kämpfer, Phys. Rev. D **95**, 125007 (2017).

[49] S. A. Smolyansky, A. D. Panferov, S. O. Pirogov, and A. M. Fedotov, arXiv:1901.02305.

[50] V. I. Ritus, J. Sov. Laser Res. **6**, 497 (1985).

[51] Y. J. Ding and A. E. Kaplan, Phys. Rev. Lett. **63**, 2725 (1989).

[52] A. E. Kaplan and Y. J. Ding, Phys. Rev. A **62**, 043805 (2000).

[53] M. Marklund and P. K. Shukla, Rev. Mod. Phys. **78**, 591 (2006).

[54] N. N. Rozanov, Zh. Eksp. Teor. Fiz. **103**, 1996 (1993) [JETP **76**, 991 (1993)].

[55] E. Lundström, G. Brodin, J. Lundin, M. Marklund, R. Bingham, J. Collier, J. T. Mendonça, and P. Norreys, Phys. Rev. Lett. **96**, 083602 (2006).

[56] J. K. Koga, S. V. Bulanov, T. Z. Esirkepov, A. S. Pirozhkov, M. Kando, and N. N. Rosanov, Phys. Rev. A **86**, 053823 (2012).

[57] A. Paredes, D. Novoa, and D. Tommasini, Phys. Rev. A **90**, 063803 (2014).

[58] F. Fillion-Gourdeau, C. Lefebvre, and S. MacLean, Phys. Rev. A **91**, 031801(R) (2015).

[59] P. Böhl, B. King, and H. Ruhl, Phys. Rev. A **92**, 032115 (2015).

[60] B. King and T. Heinzl, High Power Laser Sci. Eng. **4**, e5 (2016).

[61] S. A. Smolyansky, A. D. Panferov, D. B. Blaschke, and N. T. Gevorgyan, Particles **3**, 456 (2020).

[62] P. Bowlan, E. Martinez-Moreno, K. Reimann, T. Elsaesser, and M. Woerner, Phys. Rev. B **89**, 041408(R) (2014).

[63] N. Yoshikawa, T. Tamaya, and K. Tanaka, Science **356**, 736 (2017).

[64] M. Baudisch, A. Marini, J. D. Cox, T. Zhu, F. Silva, S. Teichmann, M. Massicotte, F. Koppens, L. S. Levitov, F. J. García de Abajo, and J. Biegert, Nat. Commun. **9**, 1018 (2018).